Journal of Scientific Exploration, Vol. 27, No. 2, pp. 205–225, 2013 0892-3310/13

RESEARCH ARTICLE

Use of a Torsion Pendulum Balance to Detect and Characterize What May Be a Human Bioenergy Field

J. Norman Hansen
Department of Chemistry and Biochemistry, University of Maryland, College Park, MD 20742, USA
nhansen@umd.edu

Joshua A. Lieberman
University of Maryland, School of Medicine, Baltimore, MD 21201, USA

Submitted 08/21/2012, Accepted 12/21/2012, Pre-published 04/25/2013

Abstract—Whereas the concept of bioenergy fields is thousands of years old, their existence has never been verified by scientific experiments designed to detect and measure them; so bioenergy fields have no scientific credibility. The instruments used for those experiments typically detect components of the electromagnetic spectrum. The experiments presented here utilize a detector that instead is sensitive to actual "pushing" forces that are capable of altering the momentum of a physical object such as a simple torsion pendulum balance that is suspended above a seated human subject. The experimental design includes a videocamera connected to a computer that can detect and measure the pendulum movements with high precision, and store this information in a data file for later analysis. Experiments show that the pendulum detects and measures substantial forces that drastically alter the motions of the pendulum when a subject is seated under it. The following effects are consistently observed with every subject in every experiment performed up to now: 1) Substantial shifts of the center of oscillation of the pendulum; shifts as large as 2.2 cm (7 deg) requiring a force that is equivalent to 45 mg are observed, 2) Many new frequencies of oscillation of the pendulum are introduced when a subject is present, 3) Dramatic changes in the amplitudes of oscillation of the pendulum are observed throughout the experiment; increasing, decreasing, and increasing again, in patterns that resemble chemical relaxation processes, 4) These shifts of the center of oscillation, the new frequencies of oscillation, and the changes in amplitudes all persist for 30–60 min after the subject has left the pendulum. This is inconsistent with the physics of a simple harmonic oscillator such as a torsion pendulum, which should return to simple harmonic oscillation immediately after any exterior disturbances are discontinued. After conducting control experiments to rule out effects of air currents and other artifacts, it is concluded that the effects are exerted by some kind of force field that is generated by the subject seated under the pendulum. We know of no force, such as one within the electromagnetic spectrum, that can account for these results. It may be that a conventional explanation for these surprising results will be discovered, but it is possible that we have observed a phenomenon that will require the development of new theoretical concepts. For now, it is important that other investigators repeat and extend our observations.

Introduction

Bioenergy and bioenergy fields have been central to the healing arts for thousands of years. However, efforts to establish the existence of these bioenergy fields using scientific instrumentation have so far been unsuccessful, so the existence of these fields is not accepted by mainstream science. This is understandable, because the scientific study of anything requires that the object of study be detectable, and that its properties can be measured, quantified, and characterized. One argument is that bioenergy fields do not exist. Another is that the instruments used to detect the biofields are inappropriate and therefore useless. An underlying assumption of heretofore biofield detection methods is that biofields consist of components of the electromagnetic spectrum and are photonic in nature. Suppose this assumption is incorrect, and that biofields do not consist of photons; in which case, previous attempts to detect these fields failed because of inappropriate detector designs. This work utilizes a detector of a completely different design. It is one that assumes that the bioenergy field, instead of being photonic, consists of a field that can exert an actual physical force; a force that can literally push against objects to alter their momentum. Since such a pushing force is likely to be small, a sensitive detector is required. A torsion pendulum, often called a torsion balance because of its ability to measure forces, was chosen because of its excellent sensitivity and simplicity. These qualities have been exploited by scientists for hundreds of years, a classic example being the accurate measurement of the gravitational constant by Henry Cavendish in 1797 (Cavendish).

Results

A depiction of the experimental setup is shown in Figure 1. The subject is seated beneath a hemispherical energy collector which is suspended by a short monofilament nylon fiber attached to a rigid support. As the detector oscillates by twisting back and forth, its motions are observed by a videocamera that is programmed to determine the position of the pendulum, usually at a rate of 10 measurements per sec, and this position information is stored in a data file together with the time of collection of each datapoint. Figure 2 shows the hemispherical energy collector, which is constructed of steel mesh, with a 1-cm white dot target attached to it, together with a screenshot during data collection of an experiment in progress. As the white dot twists toward the right, the data curve moves upward and then downward as the dot twists toward the left. Once the experiment is complete, the data file is used to chart and analyze the motions of the pendulum.

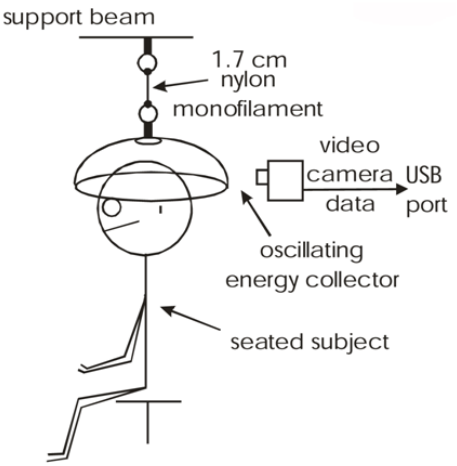

Figure 1. Subject seated under pendulum with video object-tracking camera. Pendulum components are shown in Figure 2. The camera was a ProScope Model HR2 fitted with a 1-10X lens.

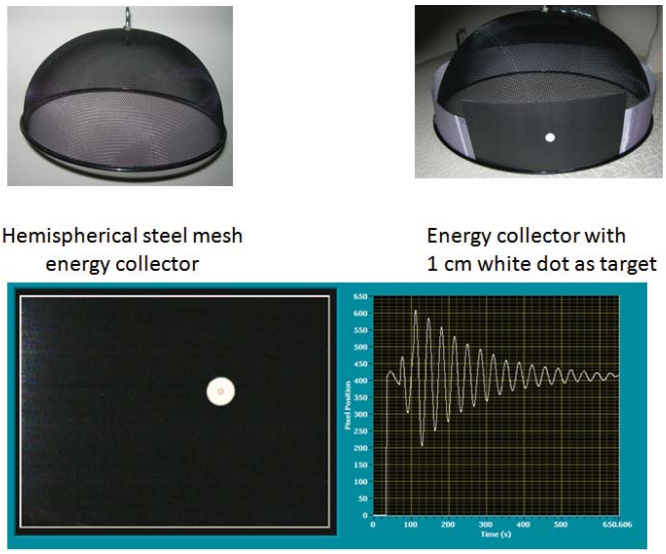

Figure 2. Components of the pendulum and data collection. The 15 x 35 cm steel-mesh hemispherical energy collector is shown on the upper left, and the 1-cm white dot target is shown on the upper right. Below is a screenshot of the data output while an experiment is in progress. It displays the position of the 1 cm white dot superimposed on a small red circle showing the calculated center of the white dot, and a graphical record of the position of the center of the white dot as the experiment progresses. The position of the center of the white dot is recorded into a data file that can be analyzed after the experiment is complete. The program for data collection was written by Irene He of http://www.hytekautomation.ca. The program can be obtained by contacting info@hytekautomation.ca.

Characterization of the Pendulum as a Classical Damped Simple Harmonic Oscillator

It is important to establish that the motions of the pendulum conform to the properties of a simple harmonic oscillator (*sho*). Figure 3 shows that it does. The graph displays two curves, one being the actual data profile obtained from the videocamera, and the other being an overlay of the theoretical curve predicted by the equation for a damped simple harmonic oscillator. This pendulum is highly damped because of air resistance and other frictional forces encountered during the twisting oscillations. Nevertheless, once a suitable damping coefficient is selected, the data curve and theoretical curve superimpose very well, even after oscillations have been highly damped. Despite the simplicity of the pendulum, its adherence to the ideal properties of a *sho* qualifies its suitability as a scientific instrument that can reliably detect forces that deflect it from its normal *sho* behavior. In its role as a torsion balance, this pendulum can also measure forces exerted against it. This requires calibration of the torsion constant of the fiber supporting the pendulum, also shown in Figure 3. The torsion constant is 2,240 dyne-cm/radian, and, using appropriate conversion factors, a force that is equivalent to 4.6 mg will deflect the pendulum by 1° of rotation. For this pendulum, a 1° rotation is equivalent to a displacement of 0.3 cm. This pendulum is therefore suitable to both detect and measure any twisting forces exerted against it by a subject sitting beneath it, if any such forces exist.

An important aspect of analysis of the motions of the pendulum is the use of the Fast Fourier Transform (FFT) to determine the frequencies of the twisting oscillations of the pendulum. The FFT analysis in Figure 3 shows that the pendulum oscillates with a frequency of 0.034 Hz, which is a period of about 30 sec.

Effects Exerted by the Presence of a Subject Seated Beneath the Pendulum

As shown in Figure 4, the pendulum detects and measures substantial forces when a subject is seated beneath the pendulum. Figure 4 shows a single continuous experiment during which the subject is seated under the pendulum during three separate time segments, each separated by a time period when the subject is absent. It is accordingly a triplicate experiment demonstrating the variation of effects exerted by the same subject during three closely spaced time intervals. Analysis of the three experimental segments reveals both consistent similarities and aspects that are different among these time periods. The behavior of the pendulum in the presence of the subject suggests the presence of an energy field above the subject.

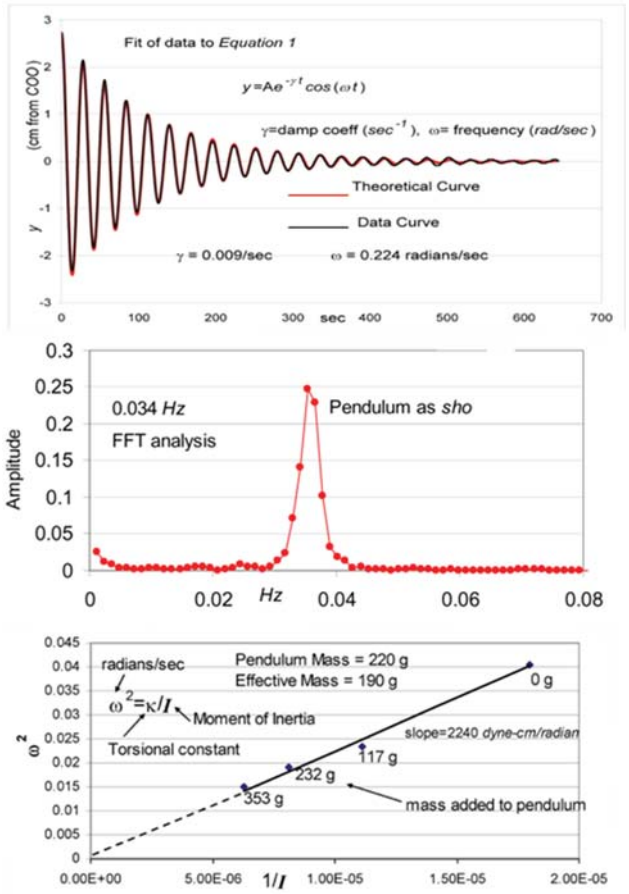

Figure 3. The pendulum behaves as a damped simple harmonic oscillator (*sho*). **(Top panel)** The black curve represents the datapoint measurements of the deflection of the pendulum from the Center of Oscillation (*COO*) taken at a rate of 10/sec. The red curve is the theoretical curve predicted by Equation 1 in which the values of ω (frequency) and γ (damping coefficient) are chosen to give a best fit to the data. The best-fit ω is 0.224 radians/sec, and the best-fit γ is 0.009/sec.
(Middle panel) FFT analysis of the data using the signal-analysis program, SIGVIEW, from sigview.com. It shows that the natural frequency of the pendulum, in the absence of a subject, is 0.034 Hz, which is equivalent to a period of 29.4 sec. SIGVIEW facilitates the use of signal-analysis principles as described by Lyons (2004).
(Lower panel) Determination of the torsional constant (κ) of the nylon support of the pendulum. The effects of adding masses to the outer rim of the pendulum on the ω of the pendulum are shown. The data are fitted to the equation shown in the figure, which gives a κ of 2,240 dyne-cm/radian, or 39 dyne-cm/deg of rotation. Using appropriate conversion factors, it was established that a force that is equivalent to 4.6 mg will displace the pendulum by 1° of rotation. For this pendulum a 1° rotation is equivalent to a displacement of 0.3 cm.

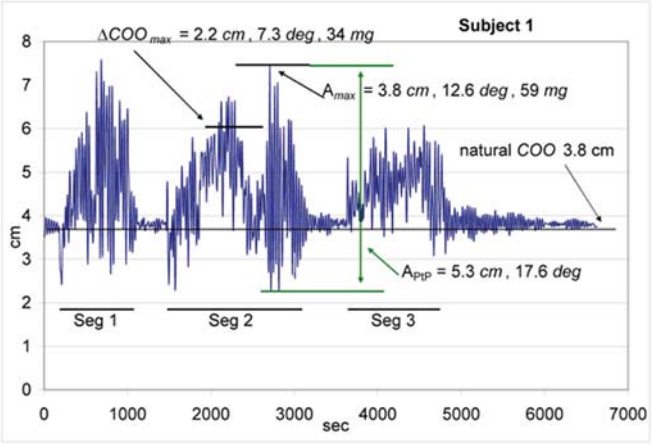

Figure 4. Patterns of oscillation of the pendulum when Subject 1 is present. The initial seconds of the experiment are twisting oscillations prior to Subject 1 being seated under the pendulum. The vertical cm axis represents movements of the pendulum in which positive values represent rotations in the clockwise direction as viewed looking downward from above the pendulum. Seg 1 is a period of time during which Subject 1 is seated under the pendulum, as are Seg 2 and Seg 3, respectively. When the Subject is present, the amplitudes of the oscillations and the Center of Oscillation (*COO*) of the pendulum both change dramatically, with the maximum Δ*COO* being indicated for Seg 2, expressed as cm, deg of rotation, and mg equivalent of force required to drive the rotation. A_{max} is the maximum amplitude of the displacement from the natural *COO* expressed as cm, deg of rotation, and mg of equivalent force. The vertical green arrow is the A_{PtP}, which is the largest peak-to-peak amplitude observed during the experiment, expressed as cm and deg of rotation. When the Subject departs from beneath the pendulum after each Seg, the pendulum reverts toward the natural *COO*, but it does not actually attain classical *sho* behavior until long after the Subject departs, as is shown in the post–Seg 3 region.

Moreover, the magnitudes of the forces being detected are substantial and easily measured, showing that it is the design of the detector that is crucial for the detection and characterization of the putative biofield.

Shortly after the subject is seated under the pendulum, which is oscillating as a low-amplitude classical *sho*, the pendulum begins to oscillate/twist with much stronger amplitudes. Moreover, within a minute or so, the pendulum begins to shift with respect to its natural center of oscillation (*COO*), and this *COO* undulates throughout Segs 1, 2, and 3. This deflection of the *COO* is substantial, and is at its highest during Seg 2, at which time the deflection is 2.2 cm, or 7.3 deg, which would require a force that is equivalent to 34 mg. This shift in *COO* does not occur in a haphazard or jumpy fashion, but

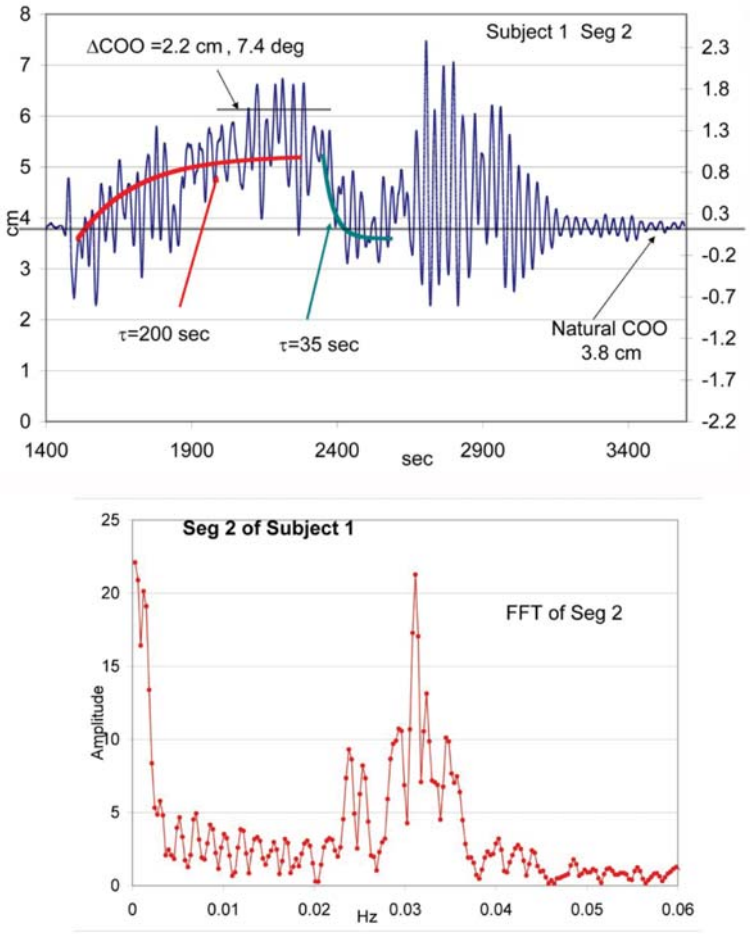

Figure 5. Focus on Seg 2 of Figure 4 data.
Figure 4 shows the results of three consecutive experiments with Subject 1 under the pendulum.
(Top panel) Focuses on Seg 2 data of Figure 4. The duration of Seg 2 is about 1,700 sec (28 min), and during that time the *COO* shifts 2.2 cm away from the natural *COO*. This corresponds to 7.3 deg of rotation, and based on the κ of the monofilament fiber would require a force that is equivalent to 34 mg.
(Bottom panel) FFT analysis of the Seg 2 data. SigView was used to analyze the frequency components that contribute to the oscillation data in the top panel. The major frequency peak is at 0.032 Hz, but there are other frequencies that are also significant. These significant frequencies encompass the entire range of 0.0–0.06 Hz (higher frequencies are small and are not shown). The frequencies that contribute to the Seg 2 profile are further analyzed in Figure 6.

occurs in a pattern that conforms to a chemical relaxation process with a corresponding relaxation constant, tau, (τ), where τ is the time it takes for an equilibrium to shift 1/*e* of the way from one position to another, and is analogous to a half-time reaction. Chemical relaxation curves are plotted on the data of Seg 2 (Figure 5), with values of 200 sec and 75 sec, respectively. That the data conform to chemical relaxation kinetics suggests that chemical principles may be useful in understanding the processes involved in mediating the shifts in the *COO*. Principles of chemical relaxations are described in Hammes et al. (1971).

Effects Exerted by the Subject on Pendulum Oscillation Frequencies

Whereas the pendulum oscillates with a single frequency when no subject is present, when a subject is present the pendulum oscillations show many new frequency components, as is shown by FFT analysis of Seg 2 in Figure 5. The largest amplitude frequency peak corresponds to the natural frequency of the pendulum, flanked by several large frequency amplitudes; and progressively smaller frequency amplitudes on both sides of the largest peak. This pattern of amplitudes is consistent with the pendulum resembling the behavior of a tuning fork that resonates most strongly with frequencies that are closest to the natural frequency. That many other frequencies that are quite distant from the natural frequency are also revealed suggests that their actual strength is substantial.

The FFT of the Seg 2 data establishes the existence of these frequencies during Seg 2, but it does not show how the strength of each individual frequency amplitude fluctuates during the Seg 2 data period. This fluctuation of amplitudes is shown in Figure 6 which employs the BandPass feature of FFT signal analysis (Lyons 2004), which allows discrete frequency ranges of the signal to be isolated and analyzed separately. The amplitude of each of the frequency ranges changes dramatically during Seg 2, with each one varying in a unique way. The actual pendulum oscillations constitute the sum of all the frequency components, according to the principles of constructive and destructive interference. The existence of many frequency components that vary among themselves and are undergoing constructive and destructive interference therefore accounts for the variability of the motions of the pendulum.

FFT Analysis Shows Substantial Differences in the Frequency Patterns of Segs 1, 2, and 3

FFT analysis of the pendulum oscillations in Segs 1, 2, and 3 are compared in Figure 7. Whereas one can see similarities, the differences among them

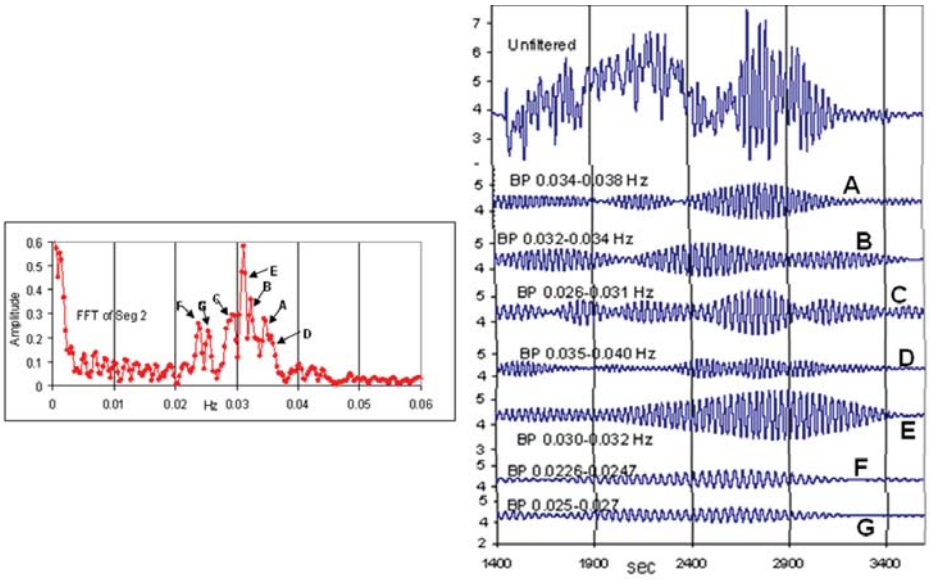

Figure 6. Frequency components that contribute to the oscillation profile of Seg 2.
(Right top panel) Shows oscillation data of Seg 2, including several min after the subject left the pendulum.
(Left panel) The FFT analysis of these data is shown.
Each of the A–G frequency peaks corresponds to a particular frequency range that is responsible for that peak. The contribution of each peak is assessed by applying a BandPass filter to the frequency range that is defined by the lowest amplitudes above and below each peak. For curves A–G, what is represented is the BandPass (BP) profile that represents the frequency contribution of that particular BP component to the top panel data, e.g., curve A is what is obtained by applying a 0.034–0.038 Hz BandPass filter to the top panel data.

are substantial; and in Seg 3 the natural frequency is greatly diminished, suggesting that the oscillations of the pendulum are dominated by the forces exerted by the subject, which override the natural properties of the pendulum.

Pendulum Motions Do Not Return to Normal until Long after the Subject Has Departed

Classical physics predicts that a *sho* that is being subjected to outside forces will immediately return to normal *sho* motion after the outside forces have been removed. Separate control experiments confirmed that this pendulum immediately returns to classical *sho* motion once outside forces such as

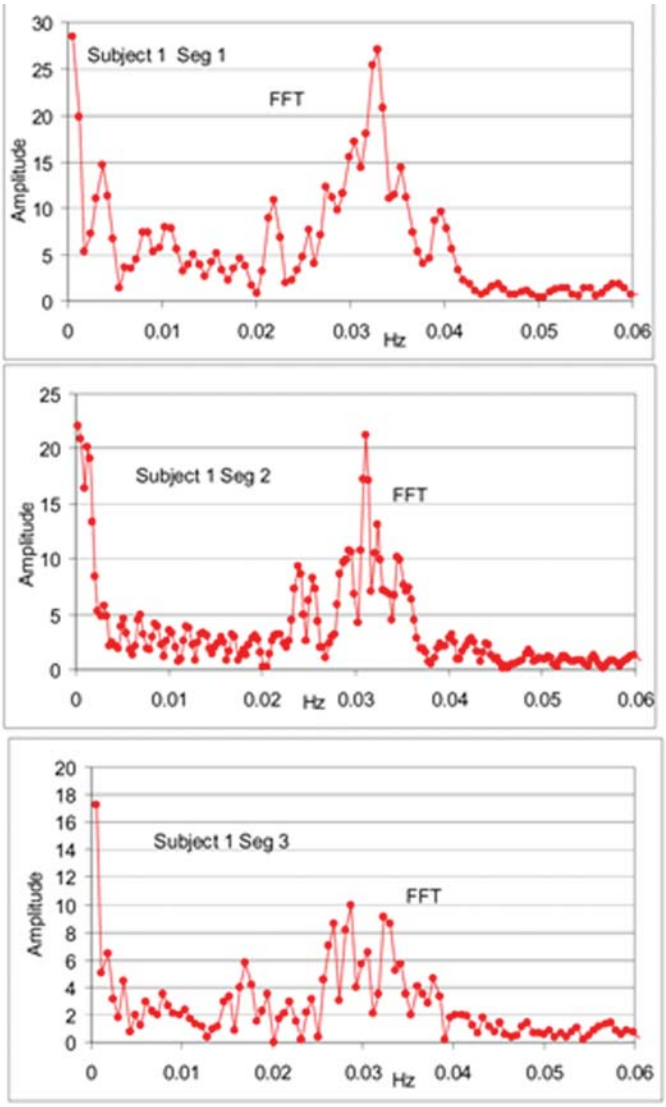

Figure 7. FFT analysis of Segs 1–3 of the Subject 1 data shown in Figure 4. The FFT profiles are aligned vertically so that differences between them can be compared. A complete analysis of the contributions of the frequency peaks in the Seg 2 FFT profile is shown in Figure 6.

puffs of compressed air have been eliminated. Inspection of the data profile in Figure 4 indicates that an immediate return to normal *sho* motion after the subject departs does not occur. This is especially evident at the end of Seg 3, when the non-classical motions of the pendulum continue to be observed long after the subject has departed. Figure 8 focuses on the time period after the subject has left the pendulum at the end of Seg 3. Two curves are shown, the red one being the expected oscillation pattern of the pendulum once the external forces have been removed, i.e. the behavior of the pendulum that is predicted from classical physics. The black curve shows the actual oscillations of the pendulum, which are very different from the expected (red) curve. Remarkably, both the deflection from the natural *COO* and anomalous amplitudes and frequencies are retained long after (30–60 min) the subject has left the pendulum. The intensities of these effects diminish with time, and the rate conforms to a chemical relaxation process with a τ of 600 sec. This is slower than the relaxation times when the subject was present, suggesting that the subject can accelerate the *COO* transitions, perhaps by catalyzing an energy-driven process, whereas the relaxation in the absence of the subject would be uncatalyzed and occur without an input of energy.

It needs to be considered that the effects observed with Subject 1 may be due to Subject 1 possessing unique abilities that result from a combination of natural talent and/or training. This possibility has been explored using many other subjects. Among more than a dozen subjects, all exert these effects, so it is neither necessary to be naturally talented nor to be trained. As an illustration, Figure 9 shows the results from the very first experiment with a new subject. In this experiment, there are shifts in the *COO* and new frequencies when the subject is present. There is also retention of the *COO* shifts and frequency components after the subject departs. Moreover, the τ when the subject is present is 200 sec, and the τ after the subject departs is 600 sec. A 200-sec relaxation was observed when Subject 1 was present (Seg 2). A 600-sec relaxation time was observed after Subject 1 departed after Seg 3. These are commonalities that suggest common explanations.

Based on many experiments using many subjects under many conditions, we are convinced that these effects are real, and not a result of experimental errors or artifacts. The most obvious artifact is air currents that are produced by the subject; a combination of body temperature, and body motion, which includes breathing. These issues were addressed by asking a subject to both suspend breathing as long as possible, and to breathe as shallowly as possible, and to reduce body motion to a minimum. These attempts had no apparent effects on the outcome of the experiment, in that substantial shifts in the *COO* and new frequencies of oscillation were

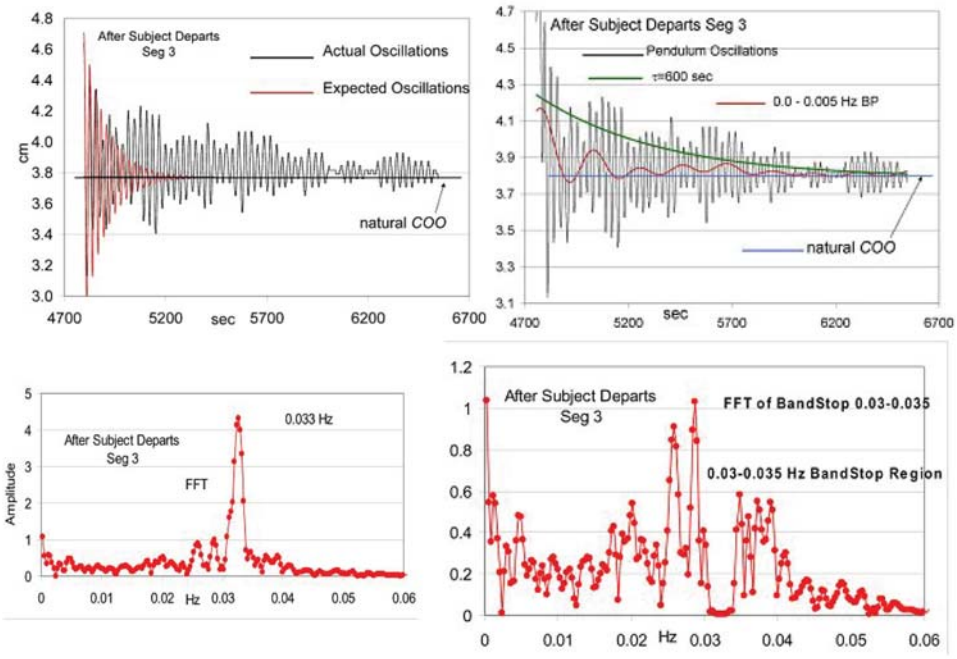

Figure 8. Analysis of region after the end of Seg 3 of Figure 4.
Subject 1 departed from the pendulum at the end of Seg 3 during a time at which Δ*COO* was still significant (~1 cm). Upon departure of the subject, the classical behavior of the pendulum should immediately resume. The pendulum did not resume classical behavior, and the deviation from expected was very large.
(Top left) The red curve shows the expected damped *sho* behavior, which is a theoretical curve calculated using the values of ω and γ obtained in Figure 3. The black curve shows the actual oscillations that were observed. It is noted that all persons left the area immediately after the end of Seg 3, so no person was in the vicinity of the pendulum during the time that these residual effects were evident.
(Top right) The green curve is the chemical relaxation curve with a relaxation time (τ) of 600 sec. The red curve is the 0–0.005 Hz BandPass frequency, which closely follows the midpoint of each oscillation during the approach to the natural *COO*.
(Lower left) FFT after Seg 3. The major peak corresponds to the natural frequency of the pendulum. Other frequencies are also present, especially the two peaks just below the main peak.
(Lower right) The continuing presence of these frequencies is made more evident by using the BandStop feature of SigView, which removes the major (0.03–0.035 Hz) fundamental pendulum frequency. Many frequencies remain, both above and below the fundamental pendulum frequency. The two frequencies immediately below the fundamental frequency have the largest amplitudes.

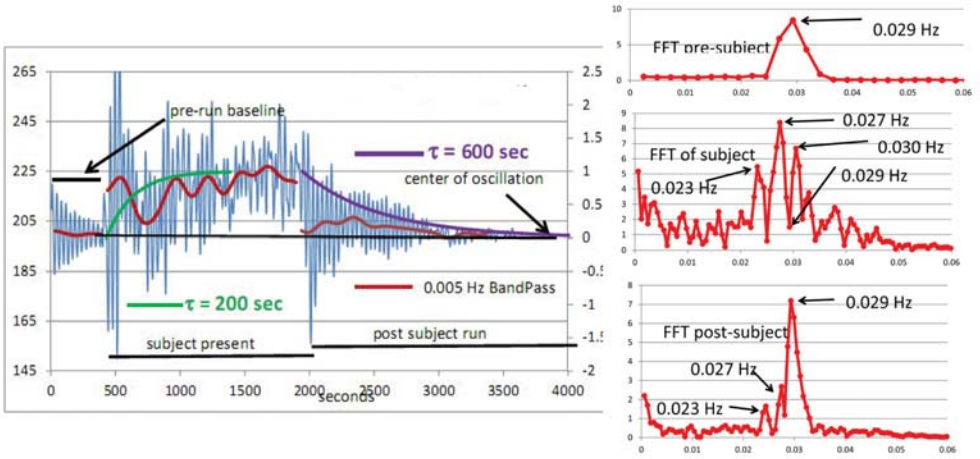

Figure 9. First experiment with a new subject.
(Left panel) The complete experiment is shown. The pre-subject baseline establishes natural *sho* behavior, and the natural *COO*. The Subject Present region is when the subject is seated under the pendulum. The post-subject region is after the subject has left the pendulum. The green curve during the time the subject is present represents a chemical relaxation process with a relaxation time (τ) of 200 sec. The red curve is the 0–0.005 Hz BandPass which closely follows the midpoint of each oscillation curve. The purple curve represents the chemical relaxation process with a relaxation time (τ) of 600 sec when Subject 1 is present.
(Right panels) FFT analysis of the three stages of the experiment.
(Top right panel) Shows the FFT prior to the subject being seated under the pendulum. The natural frequency is 0.029 Hz.
(Middle right panel) The FFT analysis while the subject is under the pendulum. Many frequencies are shown. The actual fundamental frequency of the pendulum does not appear, whereas other frequencies dominate.
(Lower right panel) FFT analysis after the subject has left the pendulum. The fundamental 0.029 Hz frequency has returned. However, the 0.027 and 0.023 Hz frequencies are still strongly present. It is clear that the effects of the subject on the pendulum persist long after the subject has left the pendulum.

observed throughout. Another experiment used a Presto-brand cooking pot with a lid that was placed under the pendulum so that the lid was in the position normally occupied by a subject. The cooking pot was heated to body temperature, and the effects on the pendulum were observed. Effects on the oscillations of the pendulum were negligible, and deviations from the natural *COO* were undetectable. These results of control experiments are available elsewhere (Hansen & Lieberman 2009).

A final concern is the possibility that the effects on the pendulum may be due to static electricity, in that static charges in the steel-mesh hemisphere could interact with static charges in the subject. This possibility was eliminated by performing experiments in which all of the components of the pendulum were connected to ground, and the subject was also connected to ground through wrist straps. The description of these experiments and the results are in the Appendix.

Discussion

These results suggest that a previously unknown human bioenergy field has been documented, which was made possible by designing a new detector of "pushing/rotational" forces that are capable of altering the momentum of physical objects, instead of the photonic detectors that have dominated in previous studies of bioenergy fields. The results appear to establish the existence, immediately above the human cranium, of a form of energy that can greatly influence the twisting motions of a torsion pendulum. Properties of the twisting force include the ability to deflect the center of oscillation of the pendulum, as well as the frequencies of oscillations. A particularly significant observation is that after the subject departs from beneath the pendulum, the effects on the pendulum are retained for a period of 30–60 min. In all of the experiments with the subject present and after the subject departs, the transitions of the position of the *COO* conform to the kinetics of chemical relaxation processes, suggesting that the principles of chemistry will be important in understanding the effects of the subject on the pendulum.

That the pendulum retains twisting-oscillatory qualities after the subject has left is reminiscent of phosphorescence, in which light can elevate electrons to an elevated state; and after removing the phosphorescent object from the light source into the dark, one can see light emanating from the object as the elevated electrons return to their ground states. The principles of phosphorescence are well-known and understood.

We hypothesize that what happens with the pendulum is similar in concept, but different in fundamental ways. It is accordingly hypothesized that the energy of the subject exerts an energy-driven effect on the pendulum that converts its atomic and molecular constituents toward higher-energy quantum states. The unusual thing is that these elevated quantum states must possess the ability to exert chiral forces that drive the pendulum to oscillate with a deflected *COO*, and also possess a kind of energy that can drive the pendulum to oscillate with new frequencies. Just as with phosphorescence, when the subject departs from the pendulum, these elevated energy states decay in a process that resembles a chemical relaxation process, which

proceeds until these elevated states are completely dissipated so that the pendulum eventually reverts to normal *sho* behavior. The experiments reported here utilized a steel-mesh energy collector. However, recent unpublished results show that similar effects are observed with a completely organic collector composed of coco-fiber. Explanations of these effects will therefore have to be inclusive of both kinds of materials.

We know of no quantum state that is capable of exerting these kinds of chiral and vibrational frequency effects. However, our results argue that these kinds of quantum states exist, and can be attained by the influence of the energy field above the subject. If so, it is very important that we study and understand this energy field. We believe that our pendulum will be a valuable component in this discovery process. While it is likely that conventional principles of chemistry, physics, and biology will provide an explanation of our results, it may be necessary to invoke exotic concepts such as quantum entanglement (Heyes, Sakuma, de Visser, & Scrutton 2009) and/or torsion fields (Kozyrev 1971).

The idea of bioenergy fields has long been a subject of derision because they have not been detectable using instruments that are sensitive to components of the electromagnetic spectrum. We have now introduced an entirely different type of detector; one which detects and measures physical forces, especially chiral forces, by means of a torsion pendulum, i.e. a torsion balance. This pendulum balance detects substantial forces on the pendulum; and the effects of these forces are highly unusual, as described in the Results section.

Unlike scientific experiments that require instrumentation that is highly complex, the pendulum described here is very simple. It is nothing more than a steel-mesh hemisphere that is suspended above the subject by a short strand of nylon monofilament. The only complexity is the measurement of the motions of the pendulum which requires a videocamera that observes the position of the pendulum over time, a computer, and appropriate software to collect the data. The data collection software is commercially available at: info@hytekautomation.ca. The simplicity of the instrumentation and the experimental procedures will allow experimenters with a wide range of interests and expertise to explore the phenomena that we have reported. In the tradition of the scientific method, it is hoped that these experimenters will test our observations by designing experiments to search for artifacts and alternate explanations of our observations. In view of the simplicity of the experiments, it is hoped that the results from other experimenters will arrive soon. We will facilitate these efforts in every way we can.

Ethics: The Institutional Review Board of the University of Maryland approved these experiments.

References

Cavendish, H. (1797). Henry Cavendish. http://en.wikipedia.org/wiki/Henry_Cavendish

Hammes, G. G., Porter, R. W., & Stark, G. R. (1971). Relaxation spectra of aspartate transcarbamylase. Interaction of the catalytic subunit with carbamyl phosphate, succinate, and L-malate. *Biochemistry*, *10*, 1046–1050.

Hansen, J. N., & Lieberman, J. A. (2009). Construction and characterization of a torsional pendulum that detects a novel form of cranial energy. http://hdl.handle.net/1903/9421

Heyes, D. J., Sakuma, M., de Visser, S. P., & Scrutton, N. S. (2009). Nuclear quantum tunneling in the light-activated enzyme protochlorophyllide oxidoreductase. *Journal of Biological Chemistry*, *284*, 3762–3767.

Kozyrev, N. A. (1971). On the possibility of experimental investigation of the properties of time. In *Time in Science and Philosophy*, Prague: Academia, pp. 111–132.

Lyons, R. G. (2004). *Understanding Digital Signal Processing*. NJ: Pearson Education/Prentice Hall. 665 pp.

Appendix
Ruling Out Static Electricity

In following through with the grounding experiments that were suggested by reviewers, we obtained important results. As you will see below, grounding of both the pendulum hemisphere and the subject had no effect on the results obtained from experiments. These experiments were done in response to concerns that the effects we were seeing might be due to static electricity, and to eliminate this possibility it was necessary to ensure that both the steel-mesh hemisphere and the subject were properly grounded.

To ground the steel-mesh hemisphere, we had to make some modifications to the equipment setup. Our original experiments were performed with the hemisphere being attached to a 1.7-cm nylon fiber support. Initial attempts to attach a grounding wire to the hemisphere resulted in the wire interfering with the oscillations of the hemisphere. The solution we chose was to substitute a copper wire in place of the nylon fiber. The copper wire was fastened to a steel eye-bolt, which was inserted into the steel mesh at the top of the hemisphere. Before attaching the eye-bolt, the mesh was thoroughly polished to brightness with emery paper, and the eye-bolt was secured with a nut on each side of the mesh, with steel washers squeezed against the mesh by tightening the bolts against the washers. Electrical conductivity between the eye-bolt and numerous locations around the surface of the hemisphere was confirmed with an ohm-meter. The other end of the copper wire support was similarly attached to the aluminum support that we normally use. A ground wire was then bolted to the aluminum support which was attached to the ground lug of a 3-prong plug, which was inserted into a grounded wall outlet.

A similar ground wire attached to a plug was used to attach to wrist straps of the type used by technicians to work with electrical equipment

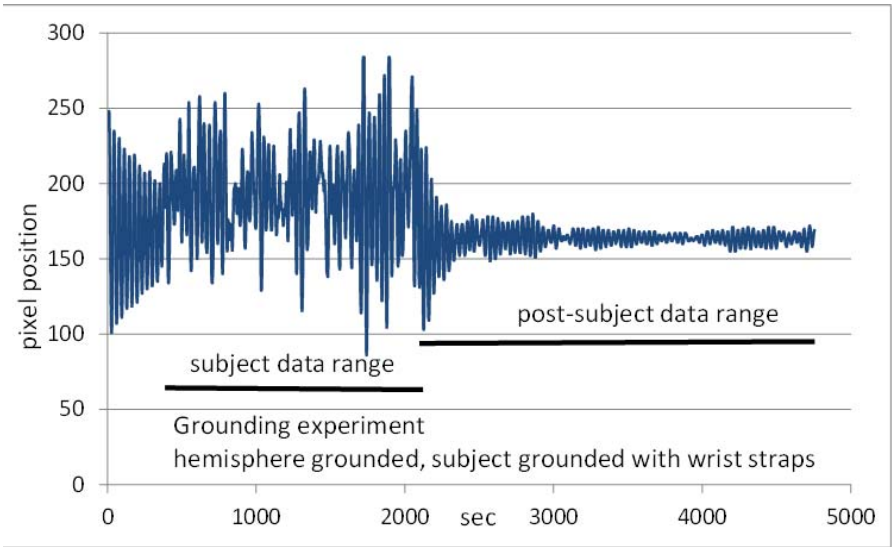

Figure 10. An experiment in which both hemisphere and subject were grounded.

that can be damaged by any static electricity that might be present on the technician. These wrist straps drain that static electricity to ground, so are appropriate for ensuring that the subject does not have a static charge. Total conductivity to ground was established by using the ohmmeter to show no resistance between the wrist straps and various points throughout the surface of the steel-mesh hemisphere.

It must be noted that the copper wire support had to be much longer than the original nylon support in order to obtain the normal 30-sec oscillation period of the hemisphere. The copper wire that gave this 30-sec period was 33 cm long and 0.32 mm in diameter, compared to the 1.7-cm, 0.7-mm dimensions of the nylon fiber. Whereas this produced the needed period, the damping coefficient was substantially smaller, so that when the pendulum was stimulated with a puff of air, it took substantially longer for the oscillations to damp down. This was due to the higher elastic coefficient of the copper metal compared with the nylon fiber. Fortunately, this did not have a significant effect on the results obtained from the experiments that were performed with a subject.

Figure 10 shows an experiment that was performed with both the hemisphere and the subject thoroughly grounded. The pendulum was stimulated in the usual way with a puff of canned compressed air and allowed to oscillate freely for 6 minutes in order to establish the natural frequency

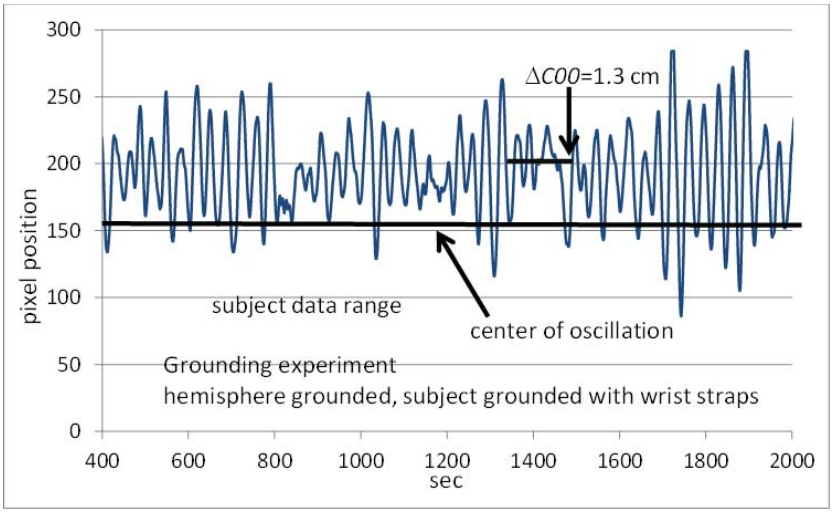

Figure 11. Pendulum oscillations during the Figure 10 time period "subject data range."

of oscillation of the pendulum. The subject then sat under the pendulum without touching it in any way. Data were collected with the subject present for about 30 minutes, whereupon the subject carefully left the pendulum and left the area. The time period when the subject was present is labeled "subject data range" and the black line shows the time period involved. The 43-minute time period after the subject left the pendulum is labeled "post-subject data range."

These data can be compared with data from the experiments in the main article in which neither the subject nor the hemisphere were grounded. They are qualitatively exactly the same, in which the "pre-subject data range" shows the conventional oscillations of the pendulum, the "subject data range" shows wild fluctuations in the oscillations of the pendulum, and the "post-subject data range" retains the anomalous oscillations for 30–60 min. To better view the oscillations that occur during the "subject data range," Figure 11 focuses on this time period.

We see the same kinds of patterns in the oscillations here as we consistently see in all of our experiments (see main article). Namely, there is a substantial shift away from the natural center of oscillation (*COO*), and there are many frequencies in addition to the natural frequency. Note that the shift away from the natural center begins immediately after the subject is seated under the pendulum, and continues to be shifted throughout the

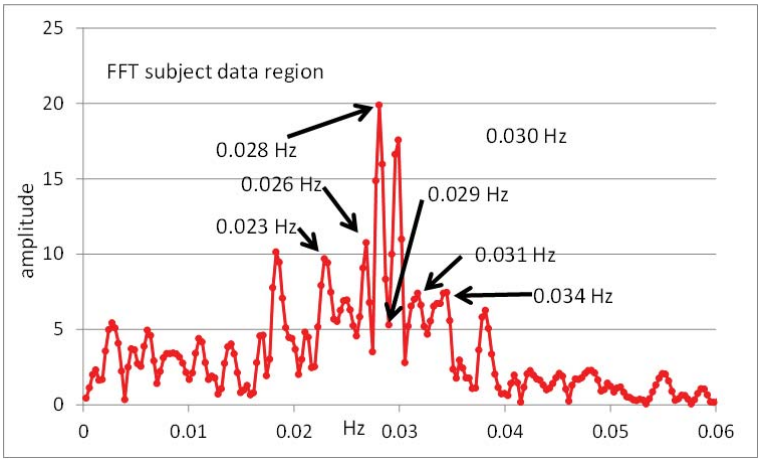

Figure 12. FFT (Fast Fourier Transform) analysis of Figure 11 "subject data range."

entire time the subject is present. The magnitude of this shift away from center is about 1.3 cm. The frequencies represented in this data range were determined by FFT analysis, shown in Figure 12.

This frequency pattern can be compared with the FFT analysis of the pre-subject data region (Figure 13), which shows just a single frequency peak, which is the natural frequency of the pendulum.

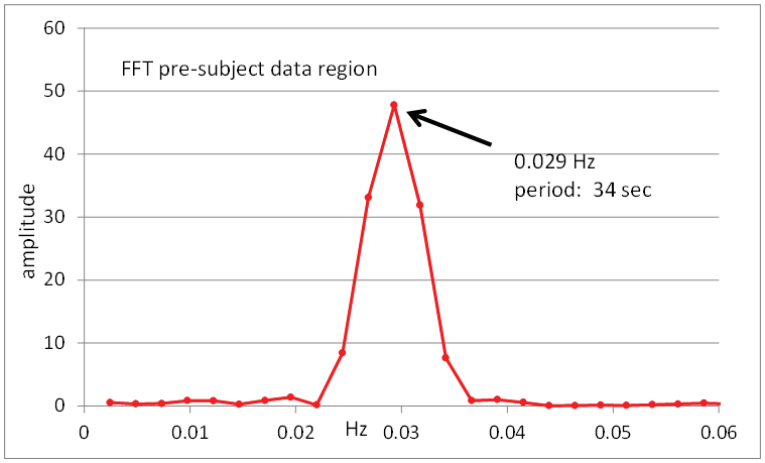

Figure 13. FFT (Fast Fourier Transform) analysis of Figure 11 oscillations in the pre-subject data range.

This experiment also shows that after the subject departs from the pendulum, the frequency patterns that were observed when the subject was present persisted after the subject departed, but at lower amplitudes. Figure 14 shows the FFT analysis after the subject departed from the pendulum.

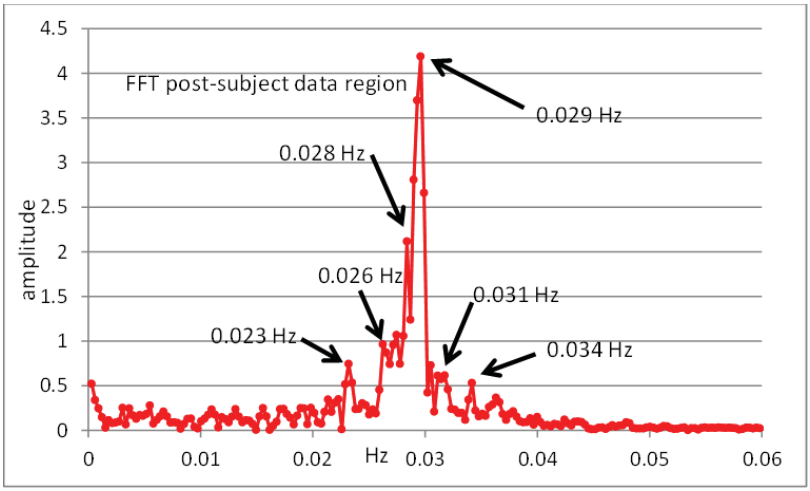

Figure 14. FFT (Fast Fourier Transform) analysis of Figure 11 oscillations in the "post-subject data range."

It is evident that the frequency patterns that were present during the time that the subject was present persist after the subject departs. This is what was observed in the experiments reported in the main article.

To show that this pattern of frequencies is unique to the presence of the subject, Figure 15 shows a run in which the same pendulum was stimulated by a puff of air, but no subject was present.

Figure 16 is the FFT analysis of this non-subject run.

We believe that these experimental results demonstrate that static electricity cannot explain the experimental results in our main article. The steel-mesh hemisphere is conductive throughout, so static charges should be distributed uniformly. Moreover, if charges were localized, it would be necessary for them to constantly move around to produce the observed results. The experiments in which both the pendulum components and the subject were grounded alleviate concerns about static charges, which should be dissipated through the ground connection, thus eliminating any static charge forces between the pendulum and the subject. Once everything has been grounded, there should be substantial differences between the grounded

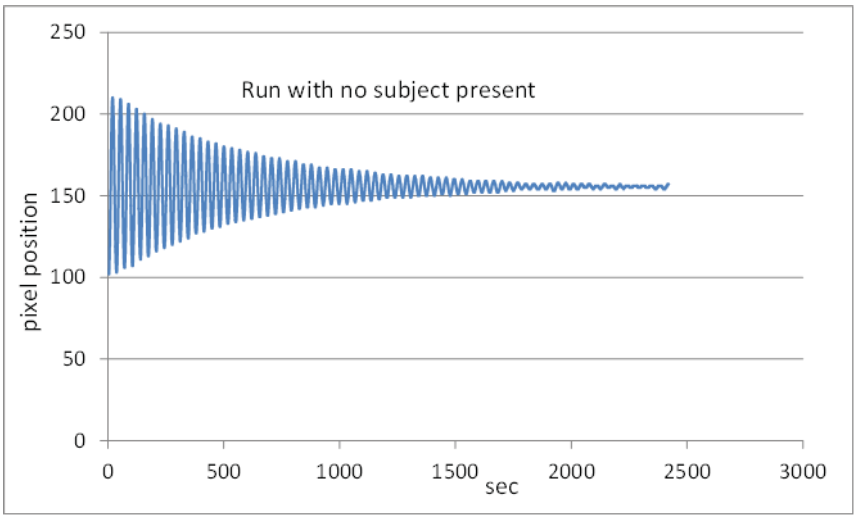

Figure 15. Pendulum oscillations in the absence of the subject.

results and the ungrounded results if static charge effects are significant. There were no significant differences in the phenomena observed in the grounded experiments versus the ungrounded experiments shown in the main article. We therefore conclude that static charges cannot explain our observations.

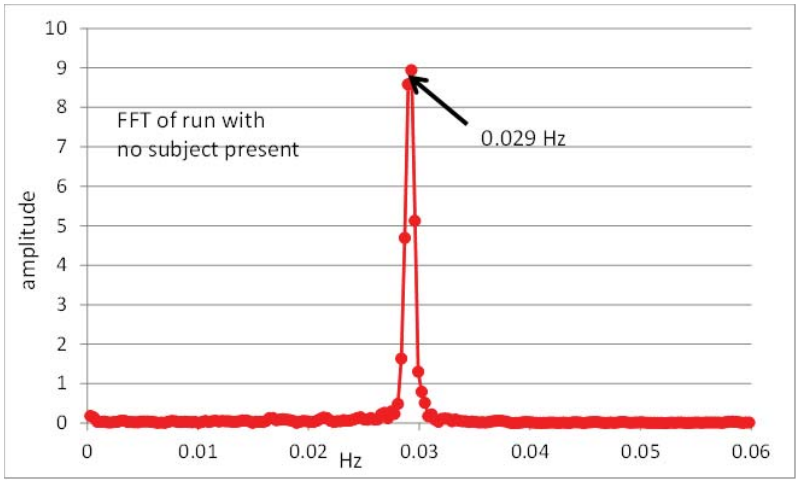

Figure 16. FFT (Fast Fourier Transform) analysis of Figure 15 data in which no subject was present.